

# Comparing Ubisense, Bespoon and Decawave UWB location systems: indoor performance analysis

Antonio R. Jiménez and Fernando Seco

**Abstract**—Most UWB location systems already proposed for position estimation, have only been individually evaluated for particular scenarios. For a fair performance comparison among different solutions, a common evaluation scenario would be desirable. In this paper we compare three commercially available UWB systems (Ubisense, Bespoon and Decawave) under the same experimental conditions, in order to do a critical performance analysis. We include the characterization of the quality of the estimated tag-to-sensor distances in an indoor industrial environment. This testing space includes areas under Line-Of-Sight (LOS) and diverse Non-Line-Of-Sight (NLOS) conditions caused by the reflection, propagation, diffraction of the UWB radio signals across different obstacles. The study also includes the analysis of the estimated azimuth and elevation angles for the Ubisense system, which is the only one that incorporates this feature by using an array antenna at each sensor. Finally, we analyze the 3D positioning estimation performance of the three UWB systems using a Bayesian filter implemented with a particle filter and a measurement model that takes into account bad range measurements and outliers. A final conclusion is drawn about which system performs better under these industrial conditions.

**Keywords**—UWB, Distance Measurement, Indoor localization, DecaWave, Bespoon, Ubisense.

## I. INTRODUCTION

Indoor localization is still an open problem. Many different approaches using distinct technologies have been proposed to obtain a usability similar to GPS outdoors [1], [2], [3]. The most difficult challenge for positioning is to find an accurate-enough indoor location method, valid for extended areas, robust to changes to environmental conditions, and at the same time as simple as possible. Different approaches can be used for indoor localization: 1) Vision-based solutions based on cameras (RGB, TOF) fixed on the environment or carried by the user [4]; 2) Beacon-based solutions using several beacons or sensors placed at known locations and one tag on the object to locate. These Local Positioning Systems (LPS) that can be implemented using trilateration algorithms or even fingerprinting techniques [5], [6], [7]; 3) Solutions that rely on dead-reckoning methods using inertial sensors installed on the person to locate (Pedestrian Dead Reckoning-PDR) [8], [9], [10], [11]; and 4) Solutions that create a mesh of radio links crossing an area with the purpose of detecting zones where a significant signal attenuation appears. This approach does not require a person to carry any device, so are commonly known as Device Free Localization (DFL) solutions [12], [13], [14].

The most accurate beacon-based LPS localization solutions are those using ultrasound [15], [16], [17], [18] or UWB radio signals [19], [20], [21]. Ultrasound LPS can reach even subcentimeter accuracies in still air conditions [22]. However, ultrasound has the drawback of a limited maximum range (about 10 meters) and can not penetrate walls, so its coverage is

limited by the number of beacons to install and the partitioning of the building. The UWB positioning systems have lower accuracy than ultrasound (about 0.2 m in LOS [23]) but has a larger coverage and ranging capability (more than 100 m in LOS). UWB can penetrate walls in buildings and can resolve individual multipath components due to its large bandwidth. Nevertheless, it is still a challenge to use UWB in indoor environments with enough accuracy and coverage [20]. The potential excellent UWB distance measurement accuracy and maximum range is in practice significantly degraded when operating indoors. The NLOS effect causes a deterioration of range measurements with larger dispersion and in-excess ranges (outliers) that could be larger than one meter in a typical usage. Also, the maximum measurable range can be reduced to less than 10-15 meters in apartment type spaces [24].

UWB technology is receiving an impressive attention in recent years for outdoor/indoor position estimation. At laboratory level, a few UWB characterization papers have been published analyzing the performance of UWB radio ranging and positioning. In [21] a performance comparison among ten impulse-radio UWB localization systems is referenced. Nine of them are laboratory set-ups that use an oscilloscope or squarer/comparator for capturing the emitted signals and estimating the TOA or TDOA. These systems use pulses with a duration between 0.25 ns to 2 ns with a 2 GHz bandwidth. The tests were conducted under small size scenarios, between 2 square meters and a maximum of  $12 \times 10$  m<sup>2</sup>. The typical error in positioning is reported between 7 and 18 cm RMS. The testing conditions are mainly LOS with static and moving robots for ground-truth definition. Apart from these laboratory solutions, few commercial UWB systems are compared. For engineering and research lab teams wanting to select COTS UWB technology it would be necessary to have access to performance comparison among commercial devices, in realistic conditions (LOS + NLOS), bigger scenarios, and under exactly the same conditions in order to get comparable and fair results.

Several commercial UWB kits are nowadays available for solutions developers and research labs to evaluate and generate their own conclusions. Among them, apart from the classical and pioneering Ubisense product, new Round-Trip UWB technologies have emerged in recent years such as those provided by Decawave and Bespoon companies. As stated above, it would be very useful for the instrumentation and measurement community to compare these UWB systems in a common framework under the same test conditions. A preliminary work has already compared, under ideal and apartment-size conditions, the performance of Decawave and Bespoon systems [24], however the Ubisense system was not included in the analysis, nor its ability to estimate position using Angle-of-Arrival (AoA) with UWB signals. In this paper we analyze, for the first time, the Ubisense, Decawave and

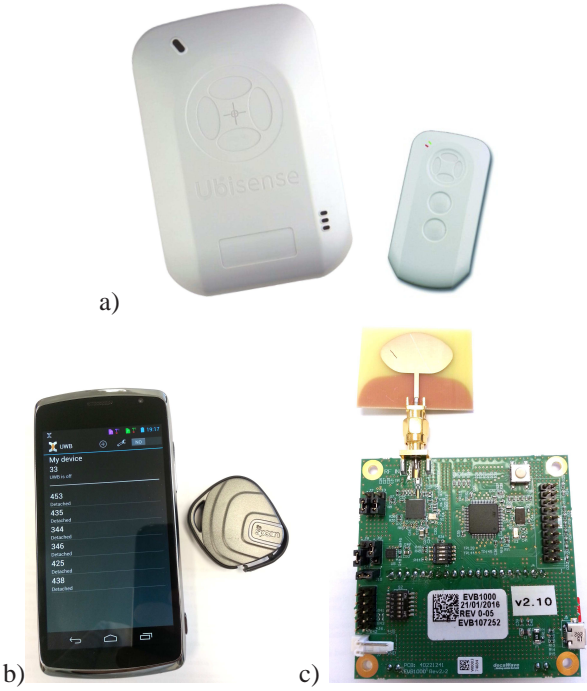


Fig. 1. UWB system under evaluation. a) UbiSense series 7000. Array antenna (left) and emitting tag (right). b) SpoonPhone and tag from the French company BeSpoon. c) Decawave EVK1000 node which can be configured as a tag or anchor.

Bespoon systems all together under the same experimental conditions. We study the range accuracy in a semi-industrial scenario, the ranging precision, as well as, the positioning performance that can be obtained with a Bayesian position estimation solution that includes NLOS and outlier mitigation.

This paper presents a description of the main features and specifications of UbiSense, Decawave and Bespoon systems in section II. The UWB range performance of all three systems and the UbiSense AoA performance is analyzed in section III. The 3D position estimation performance is analyzed in section IV. Finally, in the last section, we give some conclusions and future work.

## II. UWB LOCALIZATION SYSTEMS

This section presents the main features of the three UWB systems that we have selected for comparison: UbiSense, Bespoon and Decawave, which are the ones available at our lab.

### A. UbiSense

UbiSense is one of the first companies to commercialize the UWB technology for localization. It was founded in 2002 by Andy Ward et al., in Cambridge (U.K.). It is a leader in enterprise location solutions. It has offices in Europe (Cambridge, Paris and Düsseldorf), USA, Canada and Japan.

The UbiSense positioning system consist on a network of sensors to be installed at fixed positions, and the UWB tags whose position has to be estimated (see Fig. 1a). The sensors contain an array of antennas connected to the UWB radio receiver. The sensors calculate the location of the tags based

on reception of the detected UWB signals transmitted from the UbiSense tags. Each sensor independently determines both the azimuth and elevation Angle of Arrival (AOA) of the UWB signal, providing a bearing to each tag. The Time Difference of Arrival (TDOA) information is determined between pairs of sensors connected with a timing cable.

The company highlights that the combination of AOA and TDOA measurement techniques delivers a flexible, powerful and robust location system, enabling both an accurate location to be determined from a single sensor and a precise 3D location when only two sensors receive the signal. So, AOA and TDOA integration can be used to minimize infrastructure and installation costs or to improve the reliability and robustness of the system.

The ultra-wideband RF channel is within the 6-8 GHz band. There is an additional narrow-band telemetry channel at 2.4GHz, which support two-way control and telemetry communications with UbiSense tags (monitoring battery, button, leds etc.) According to the manufacturer, the maximum operating range, for the UbiSense 7000 sensor type (the one used in this evaluation), is greater than 160 m and the achievable accuracy is better than 15 cm in 3D. The tag update rate can be set up between 0.1 and 20 Hz. A kit with 6 sensors and 10 tags costed to us 26,900 euros (VAT and shipping included).

### B. BeSpoon

Bespoon is a French start-up company which has developed a miniature IR-UWB system. They were the first manufacturer to demonstrate that UWB technology can be successfully integrated into a smartphone. The SpoonPhone is a prototype that has been sold to hardware manufacturers and software developers for research and evaluation purposes. One phone plus 6 tags costed to us 1,699 euros (VAT and shipping included). Now they changed the sale strategy and their products are sold as general purpose modular kits (UM100) to design your desired solutions. These modules offer the possibility to achieve good precision (down to 10 cm), ranging (up to 880 m in Line of Sight) and receiver sensitivity (down to -118 dBm). It uses UWB channel 2 (3.99 GHz).

The UWB radio can be activated in the SpoonPhone in the same way the WiFi/BLE radio is enabled in a phone, i.e. by switching it on at a menu (Fig. 1b). The UWB antenna is also used for WiFi communication, and it is located top-left when looking at the phone's screen. An SDK API is made available to programmers so as to access in real-time to the ranging data from the phone to the different miniature tags. The average rate of range measurements is 2.5 Hz.

### C. DecaWave

Decawave DW1000 modules are fully integrated low power CMOS chips, compliant with the IEEE 802.15.4-2011 Ultra-WideBand (UWB) standard. They make it possible ranging measurements with an accuracy of  $\pm 10$  cm using two-way ranging (TWR) time-of-flight (TOF) measurements. The manufacturer estimates a real time location accuracy for a moving tag of about  $\pm 30$  cm in X and Y; using either two-way ranging (TOF) measurements or one-way time difference of arrival (TDOA) approaches. A maximum measurable range of 300 meters is possible in ideal conditions.

This company provides the TREK1000 development Kit. One kit costs 925\$ (importation custom charges apart). The kit contains 4 fully functional UWB nodes (see Fig. 1c), which consist of a DW1000 UWB ranging chip, a processor STM32F105 ARM Cortex M3 and a omnidirectional antenna. The nodes are able to connect among them and estimate their inter-node ranges. An external device (PC) can be USB connected to any of the nodes to collect all inter-node ranges.

Each UWB node can be configured as an anchor or as a tag, by changing the dip-switches available on PCB board. Also using the dip-switches it is possible to select among two channels (2 and 5), respectively at central frequencies (3.99 GHz and 6.48 GHz), and 2 data rates (110 kbps and 6.8 Mbps). By default the configuration settings are: 4GHz as central frequency and 110 kbps data rate. This data rate is the recommended configuration for maximum distance measurement. According to manufacturer, a ranging update rate of 3.5 Hz is expected for one moving tag (update rate is lowered as the number of tag is increased since they are time multiplexed).

### III. UWB RANGING PERFORMANCE

This section describes the testing scenario, the performance in ranging (relative for Ubisense and absolute range in case of Decawave and Bespoon), and the unique bearing information provided by the Ubisense system.

#### A. Testing Scenario

In our previous work [24], we already tested the Decawave and Bespoon systems under ideal LOS conditions and in a small apartment. The present paper aims to extend previous work by exploring the behavior of UWB technology in a bigger size industrial warehouse containing diverse obstacles. The testing scenario, the “Nave” building of the Centre for Automation and Robotics (Spain), causes the propagation/difraction of UWB radio signals across different obstacles (such as, vehicles, robots, rails, frame structures and diverse instrumentation), as well as furniture, metallic cabinets and the outer brick walls of this indoor scenario. The photos shown in Fig. 2 help to understand the testing conditions.

As seen in Fig. 2, we installed 6 UWB beacons at fixed positions for each of the three UWB systems. The exact X-Y position of each of the six nodes is: [0 0; -7.7 0; -17 0; -16.8 13.8; -7.8 13.8; 0 13.8]. A slight difference in height installation exists among the 3 systems due to space restrictions. The height was 2.32, 2.48 and 2.60 m above the floor, respectively for Ubisense, Bespoon and Decawave nodes. Note that there is no diversity in the installed Z coordinate (same height), so if trying to estimate the localization of tags, a double solution appears above and below the plane defined by beacons. Our experiments with the mobile tag will be limited to heights below 2 meters, so no ambiguity is created. In fact we made experimentation keeping a constant height of 0.76, 0.72 and 0.85 for Ubisense, Bespoon and Decawave tags, respectively. That Z coordinates for tags correspond to the height of the stool used plus the height of the node’s antenna itself. See Fig. 3 for a picture of the mobile tag position and orientation on the stool.



Fig. 3. Mobile nodes on top of the stool that was used for data collection.

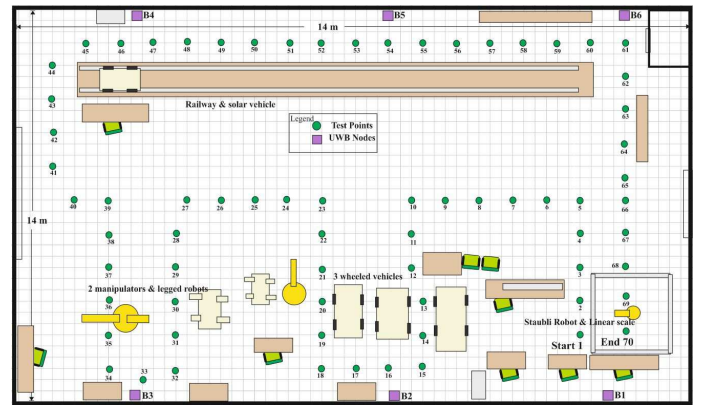


Fig. 4. Industrial indoor space (“Nave”) where measurements took place. A total of 70 test points were selected (green numbered circles). The testing points are selected to generate diversity in ranges to beacons and also passing close to disturbing objects in the environment.

The experimentation consisted in moving one mobile node to 70 different ground-truth positions. This experimentation was repeated 3 times for each of the UWB systems. We did not perform the data capture in parallel for the three systems because they can interfere each other as already detected and commented in [24]. A map of the testing area is shown in Fig. 4, where it can be seen the floor plan with the detailed anchor positions and the distribution of the 70 test points. The grid on the floor corresponds to real tiles of size 40 × 40 cm. We used this tiling partitioning to define the 70 ground-truth test points with enough accuracy, i.e. better than 2 centimeters ( $\pm 1\text{cm}$ ), which is the joint error that we estimate comes from tiling and manual stool positioning. The time in each test point was 30 seconds, so each tests lasted 35 minutes (i.e.  $30 \times 70 = 2,100$  seconds).

A transition from a position to the next one was done manually, so to guarantee a good ground truth, we rejected 7 seconds before and after each displacement. So, from a total of 2,100 seconds, we only took into account as ground truth, 1,120 seconds (16 s × 70 out of 30 s in each position). Figure 5 shows the different ground truth intervals at each of the 70 positions, at different ranges from the six anchors (in different colors). The measured distances should be as close as possible to these GT ranges in order to be as accurate as possible.

As we can observe in Figure 5, the experiment is designed to provide a full variety of different ranges. In this set-up



Fig. 2. Industrial environment used for testing the UWB systems. Dimensions 24 by 14 meters ( $336 m^2$ ). Six UWB beacons (marked in yellow circles) for each of the three UWB system are installed to cover the whole indoor area.

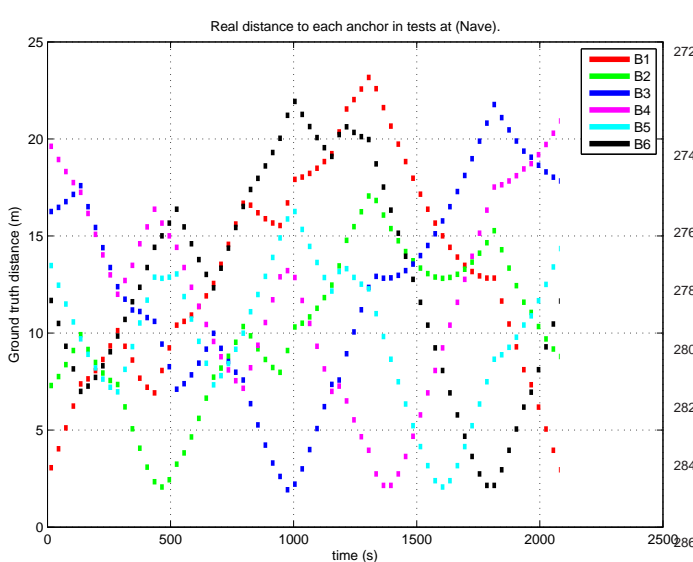


Fig. 5. Real distance to each anchor for each of the 70 testing points. Each color represents the distance from the mobile node to each of the six sensors. The experiment (2,100 seconds long) is split into 70 testing positions of 30 seconds each. The colored line fragments in this figure are 16 seconds long and are centered within each 30 second testing period. Only these time-limited ranges are used as ground-truth (GT) for ranging performance evaluation.

270 we get as close to beacons as 2 meters (that includes height  
271 difference between tag and anchor) and the further distance is  
272 23 meters (diagonal from a test point at the periphery to the  
273 opposite corner anchor).

#### B. Ranging error

274 Using the test setup described above, we compare in this  
275 subsection the absolute ranges measured by Bespoon and  
276 Decawave systems with the GT ranges presented in Fig. 5.  
277 In the case of the Ubisense system that operates by TDOA,  
278 no absolute ranges are available. In this case in order to obtain  
279 comparable measurements we added to each of the 5 TDOA  
280 values the GT range of anchor number 1 (the one configured as  
281 master and reference). The TDOA is obtained from one of the  
282 low level fields recorded as a logfile in the Ubisense location  
283 engine.

284 The theoretical sources of error in UWB ranging are due  
285 to propagation effects, clock drifts in nodes and interference  
286 with other external radio sources [25]. The propagation effects  
287 can be caused by severe multipath and by propagation delays  
288 due to the propagation of signals within blocking materials. In  
289 case of moderate multipath with a weak but detectable direct  
290 path, UWB is capable of correctly measuring the LOS time  
291 of arrival. However when the direct path is blocked, then the  
292 measured ranges corresponds to the shorter NLOS path that  
293 could include a significant delay from a few decimeters to

several meters. Taking into account that the relative electrical permittivity ( $\epsilon_r$ ) of common materials are between 2 and 6 for radio frequencies between 2 and 10 GHz, then the distance delay,  $\delta r$ , is the apparent extra range that appears when a signal propagates through a material. This extra range error  $\delta r$  is proportional to the material thickness and to the square root of material's permittivity:

$$\delta r = (\sqrt{\epsilon_r} - 1) \times \text{thickness}. \quad (1)$$

The extra range error caused by straight propagation throughout a blocking materials, such as a wall, is therefore relevant, but limited by the typical thickness of walls and indoor obstacles, i.e. expected  $\delta r$  are about 10 to 40 centimeters. This direct error caused by propagation throughout an obstacle, is in many cases not so important as the range errors caused by multipath propagation (direct path blocked but alternative longer path between emitter and receiver exist). Under these multipath cases with blocking direct path transmission, as said above, errors of several meters can be found.

In order to compare the theoretical expected error values with the experimental ones, we plotted the relationship among the real and measured distances for the three systems in Fig. 6. It can be seen that the measured ranges are not ideal like in the LOS case presented by [24], so there are ranging errors between a few centimeter until 1-2 meters in the most precise systems (Decawave and Bespoon). The Ubisense range results are much more noisy with errors larger than 10 meters in many cases.

The positive aspect of all these errors is that the dispersion is almost always in excess, which is the ideal behavior, i.e. there should never be range measurements shorter than the real straight signal path. Unfortunately, we detected some few cases in all three systems were they generated ranges shorter than the real distance. This unexpected behavior, that can not be explained by multipath, could be probably caused by multiple-access interference, or maybe due to some peak detection or filtering problems in the software libraries or hardware. As opposed to the Decawave findings in [24], where no shorter ranges than LOS were found, now we have found these kind of error in all systems as shown in Fig. 6.

The ranging error (measured range minus true range) is shown in detail in Fig. 7 as a histogram with the number of occurrences for different range errors. We can see in this figure that Ubisense system has a long tail of errors larger than 30 meters. The percentage of valid measurements are only 30% and of them half of measurements are in the long tail and another half normally distributed with zero error and a standard deviation of 1 meter. Taking into account the best ranging systems, the Bespoon errors are slightly larger than those for the Decawave system, but in any case the error distribution is similar. There is a low-sigma Gaussian distribution ( $\pm 0.15m$ ) around zero error (LOS paths in the indoor setup), and additionally a significant tail distribution (almost exponential) along the positive error side. The length of these tails, 1.2 m for Decawave and 2 m for Bespoon, corresponds to the in-excess ranges caused by NLOS direct path blockage and obstacle propagation delays. Of course, the absolute length value of this error tail will depend on the

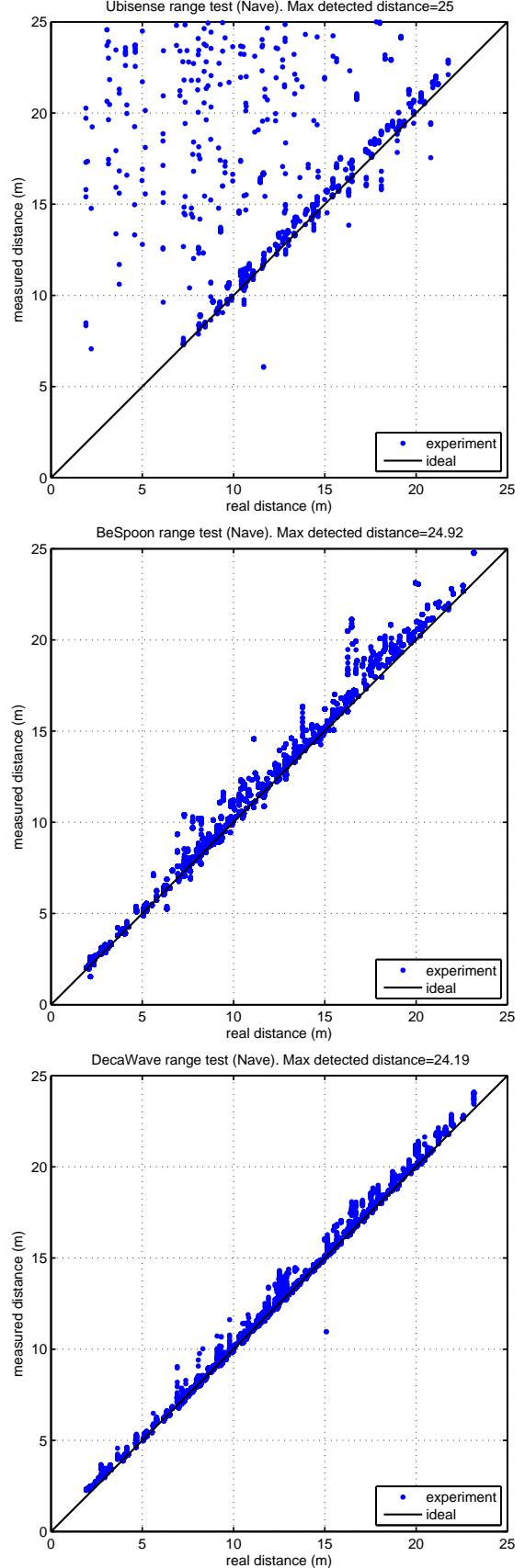


Fig. 6. Real versus measured distances in industrial indoors conditions, using the UbiSense (top), BeSpoon (middle) and Decawave (bottom) systems.

particular experiment and severity of NLOS conditions, but it is important to highlight that the tail is slightly shorter under the same experimental conditions for the Decawave system (same conclusion as in [24]). On the other hand, the negative range errors to the left half in the histogram (i.e. outliers at shorter distances than straight or LOS path) appear at all systems but are not too frequent.

The error distributions shown in Fig.7 represent the measurement models that should be applied, when designing a localization system, to alleviate the impact of in-excess ranges in localization estimation.

### 362 C. Ranging precision

Last subsection explored the accuracy in ranging, that is the error with respect to the true range. It is also of importance to the instrumentation and measurement community to analyze the precision of measurements, i.e. the repeatability or variance of estimations. In previous works, the experimental characterization and modeling of UWB ranging system has been presented [26], [21]. In those studies, the ranging technique was based on thresholding and energy detection over impulse UWB radio pulses, so ranging at larger distances causes larger pulse attenuation and therefore a predictable larger bias and standard deviation. The characterization made in [26] was restricted to a maximum of 9 meters and for LOS conditions. Our study will also try to verify that predictions and conclusions from that work and extend the testing to ranges up to 25 meters and NLOS conditions.

In order to perform the analysis of the variation in the standard deviation as the tag to sensor distance changes, we have split our testing ranges (from 0 to 25 meters) in five intervals of 5 meters each (0-5, 5-10, 10-15, 15-20 and 20-25 meters). In order to compute the standard deviation we have previously removed the more clear outliers from the estimated errors (those errors larger than 1 meter). Figure 8 shows a bar graph with the range standard deviation for the three UWB systems under comparison. As the theory predicts, there is a slight but significant dispersion increase when the distance among tag and sensor grows. Decawave standard deviation goes from 0.13 to 0.23m for ranges intervals going from 0-5m to more than 20 meters. A similar behaviour is detected for Bespoon and Ubisense, going from 0.21 to 0.28 and 0.3 to 0.63 meters; respectively.

### 394 D. Complementary AoA measurement for Ubisense

As described in section II-A, Ubisense location estimation is based on the fusion of TDOA (Time Difference of Arrival) and AOA (Angle of Arrival). In last section we showed that TDOA measurements were quite noisy and full of outliers. In this subsection we are presenting the capability of the Ubisense system to estimate the AOA in terms of the azimuth and elevation. The same testing scenario and measurements against its ground-truth allow us to analyze its reliability. In Fig. 9 we shown the azimuth estimation results.

We can observe in the title of Fig. 9b that the azimuth estimation is available in 75.4% of measurements. As seen in the histogram for all the valid measurement, less than 10% of measurements are outliers (RMSE error of 18.5 degrees). The rest of azimuth measurements (those within an absolute

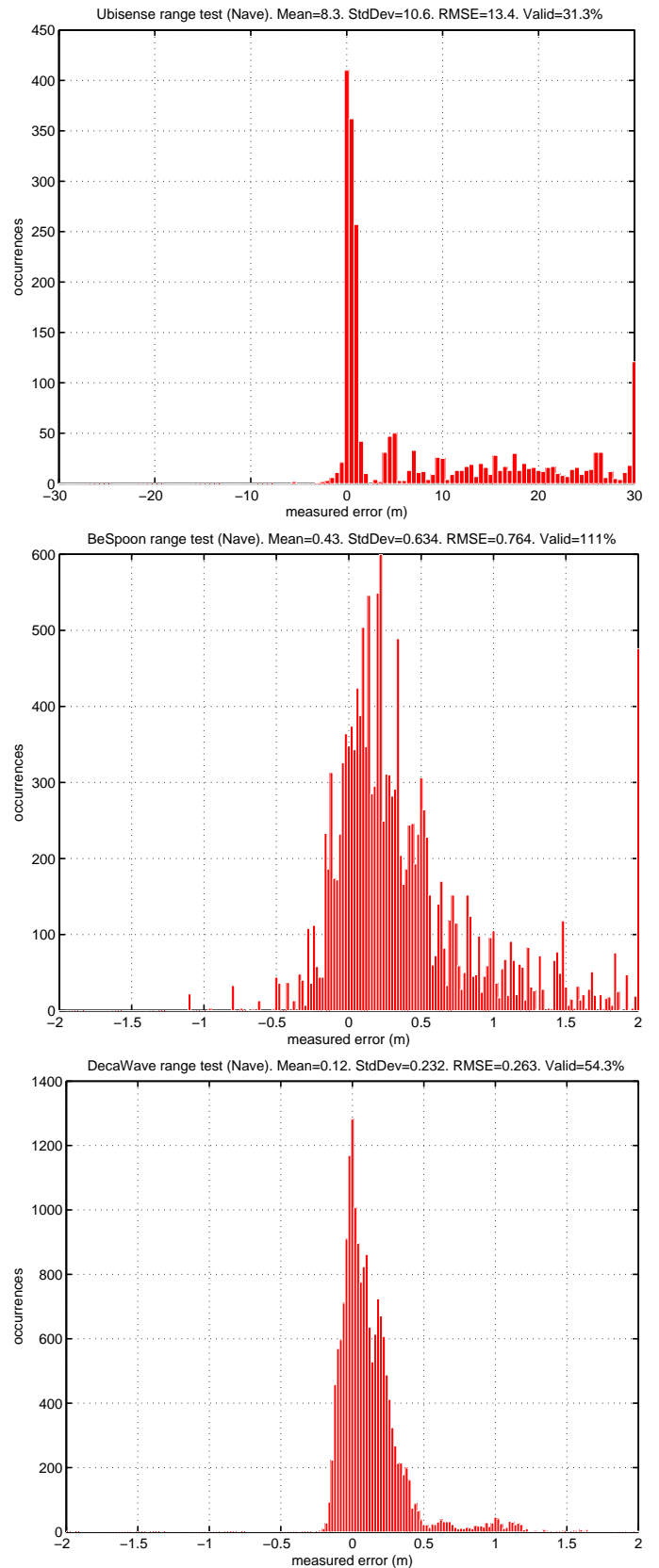


Fig. 7. Histogram of range error, in industrial indoors conditions, using the Ubisense (top), Bespoon (middle) and Decawave (bottom) systems. Note that top (Ubisense) abscissa axis are at a much higher scale than the lower ones.

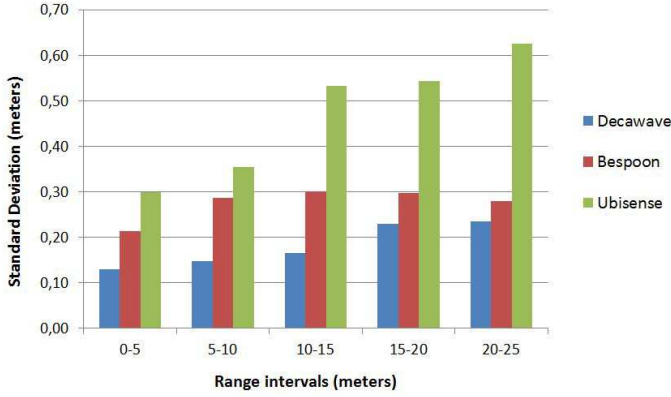


Fig. 8. Standard Deviation of range errors for different distance intervals. Outliers have been removed from the standard deviation calculation.

408 error below 10 degrees) are normally distributed with almost a  
 410 zero mean error (1.1 degrees) and a standard deviation of 5.4  
 412 degrees. Note that the experiment is quite challenging since  
 414 it includes the whole range of azimuth angles from -90 to 90  
 degrees. The error amplitude is not correlated with the azimuth  
 values, so the normal deviation and outlier content is similar  
 in the whole -90 to 90 range.

416 Regarding the elevation estimation, the range of tested  
 418 values goes from +4 to -58 degrees, for far away tags and  
 420 very close to sensor cases, respectively. We can see in Fig. 10  
 422 that the number of outlier is not too high but the accuracy  
 424 of the estimation is poor (RMSE error of 10.6 degrees) in a  
 426 64-degrees range. These results indicate that the Z location  
 428 coordinate of the tag can not be determined reliably.

422 After analyzing the quality of the whole TDOA and AOA  
 424 estimations for Ubisense, we now understand why it is so  
 426 necessary to integrate all this information in order to fill gaps,  
 remove outliers and smooth the trajectory of the moving tag.  
 Next section will present the localization results using the 3  
 428 UWB systems.

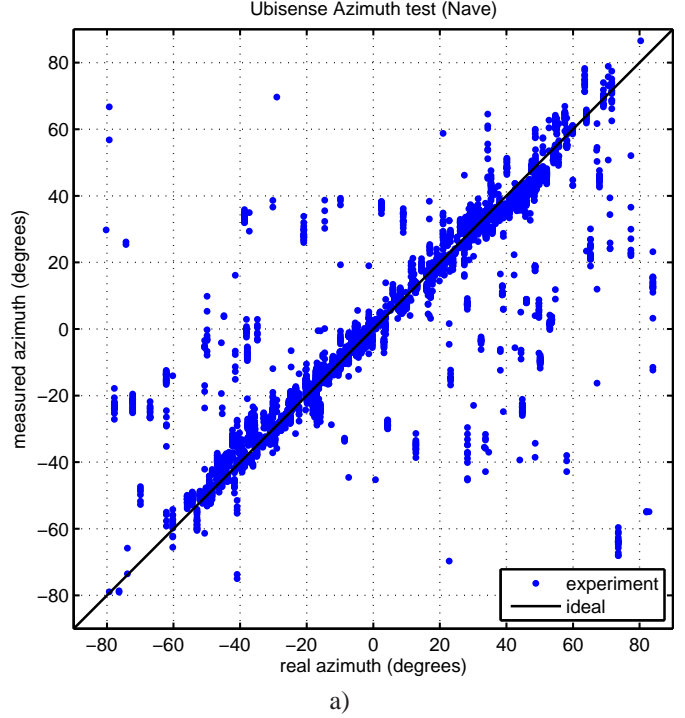
#### IV. POSITIONING PERFORMANCE

430 This section uses the available UWB ranging information  
 432 from the three systems to estimate by trilateration the 3D  
 434 position of the moving node. In the Ubisense case the absolute  
 436 range is not available, but the TDOA. As a valid time reference  
 438 is missing in the Ubisense logfiles, we add the real distance  
 440 from the reference sensor to each known test position to  
 442 compute the absolute range.

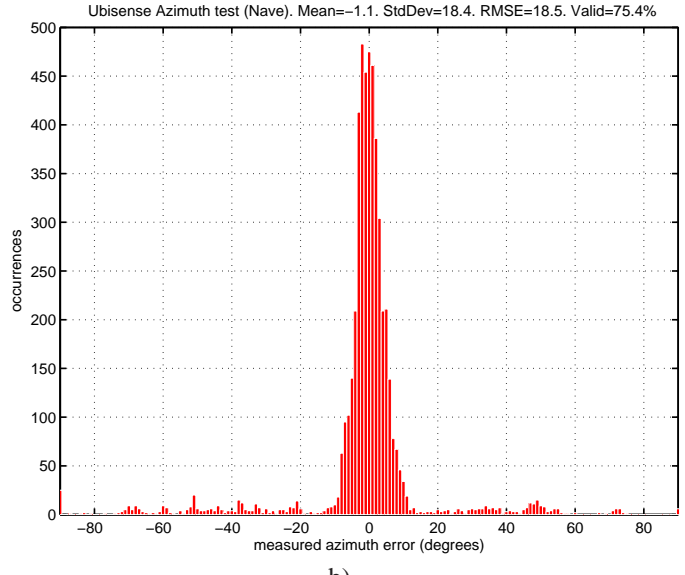
436 The 3D positioning estimation using absolute ranging data  
 438 for the 3 systems, was done using a Bayesian filtering approach  
 440 based on a particle filter. This filter is exactly the same that  
 442 the one presented in [24]. This method uses as measurement  
 444 model the error histograms presented before in section III-B  
 446 to mitigate NLOS measurements.

##### A. Positioning approach with NLOS mitigation

444 As already discussed in [24], there are several methods  
 446 already proposed for NLOS error mitigation in positioning  
 448 systems. As this paper just want to do a positioning perfor-  
 450 mance comparison between UWB systems, we will use one



a)



b)

Fig. 9. Azimuth estimation for Ubisense system. a) real vs. estimated azimuth; b) azimuth error distribution by means of an histogram.

of the state-of-the-art NLOS mitigation methods. The focus of this section is to explain the positioning method used and the reason for using such a NLOS mitigation method.

There are several approaches for NLOS mitigation: 1) Those who assume a moving target that generates a larger standard deviation of measured ranges under NLOS conditions [27]. Therefore, assuming a calibrated LOS measurement model, any range measurement sequence with a larger standard deviation is considered affected by NLOS and can be rejected before the trilateration stage. 2) A second NLOS approach makes use of the UWB signal waveform, analyzing the peaks

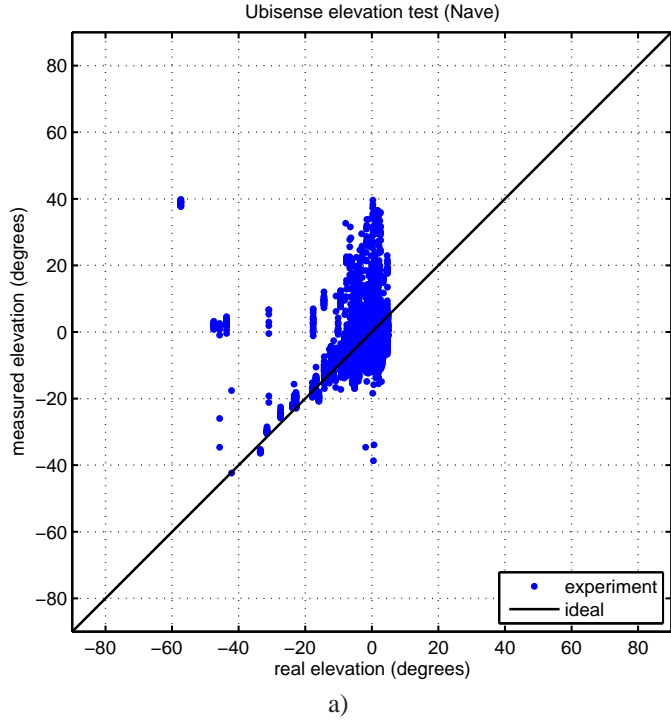


Fig. 10. Elevation estimation for Ubisense system. a) real vs. estimated azimuth; b) azimuth error distribution by means of an histogram.

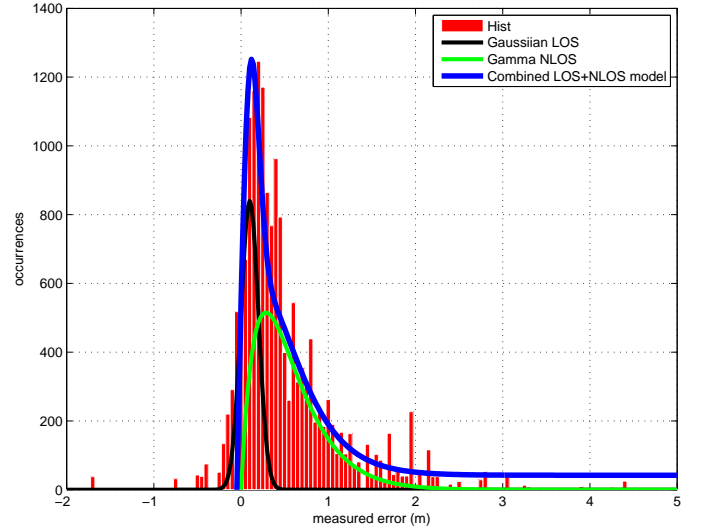


Fig. 11. Measurement model used for trilateration (blue plot) that corresponds to equation 2. Histogram data points in red are for Bespoon phone.

that can adapt to skewed and heavy-tailed measurements distributions [30], [31]. Instead of using Gaussian assumptions they model range error by mixtures of Gaussians [32] and skew t-distributions or log-normal distributions, whose model parameters can even be updated in real-time to fit the severity of the NLOS conditions [33], [34].

In our case we can not make the assumptions needed in the first three methods listed above (no motion, no waveform, no enough redundancy), so we will rely on the fourth mitigation approach. We use a tailed UWB-ranging measurement model fitted to the experimental measurements seen before in Fig. 7 in last section.

A simple long-tail measurement model for NLOS conditions is the exponential distribution. In our case we will use a model, as already proposed in [24], that combines a Gaussian distribution (for the LOS measurements) and a Gamma distribution (for the NLOS cases) and a constant value to cope with additional uncertainty and spurious measurements. This measurement model,  $f(x)$ , is explicitly stated as:

$$f(x) = \frac{1}{\sigma\sqrt{2\pi}} e^{-\frac{(x-\mu)^2}{2\sigma^2}} + \lambda \cdot e^{-\lambda x} \cdot \frac{(\lambda x)^{k-1}}{\Gamma(k)} + cte \quad (2)$$

where  $x$  is the range measurement error,  $\sigma$  is the standard deviation in LOS conditions,  $\mu$  is equal to 0.1 m, and for modeling NLOS  $\lambda$  is 3.5 and  $k$  equals 2. The last term,  $cte$ , is equal to a 3% of the model's peak. Those parameters were found fitting the model to experimental data. The representation of this combined LOS+NLOS model is displayed in Fig.11 with a blue line. It corresponds to the addition of the LOS Gaussian distribution (black line), the NLOS Gamma distribution (green line) and a constant term.

It is important to say that the distribution  $f(x)$  (eq.2) admits large spurious measurements (without limit), so strictly speaking it can not be considered a probability density function having a normalized unit area. In fact, as we will present next,

and strength of the first and the secondary peaks in the signal [28]. It is possible to do an optimal selection between the thresholds and the time interval of neighboring peaks in order to select the most likely range. 3) Other assumes that there is a redundant number of beacons for trilateration, so it is possible to apply robust filtering techniques [29], for example selecting several subgroups of beacons, and getting the solution with a larger consensus. This approach to be successful must satisfy that the number of affected NLOS ranges is lower than the number of LOS ranges. 4) A more flexible and general purpose approach tries to find probability distribution models

502 during the particle filter measurement update implementation, this non-normalized distribution function  $f(x)$  will be used, but always followed by a normalization of all particles weights.

504 It is also important to highlight that the  $f(x)$  model  
506 parameters under use are the same as the ones used in [24], in  
508 that case for a different experimental setup. The idea is also  
to test and compare the model validity and generality for a  
different scenario.

510 The particle filter with 3 spatial states (i.e. X Y and Z)<sub>560</sub>  
512 is used to do the position estimation by trilateration with  
measured ranges. A total of 2,000 particles are used, which are  
514 initially distributed at random positions within the workshop  
area. No motion information is available (no wheeled or  
516 pedestrian odometry), so in our particle filter the motion  
capability is generated with a random particle dispersion once  
518 every second. This random particle dispersion is used to let  
particles to move from one position to other and consequently  
520 to track the motion of the moving node. The particle filter do  
not estimate direction or orientation of the moving node, just  
3D XYZ coordinates, so the only way to move particles is to  
522 use this motion model that assumes that a person can move  
walking at a speed of approximately 1 meter per second. <sub>572</sub>

524 Once a range measurement to a beacon is available, then<sub>574</sub>  
526 the real distance among all particles and that beacon are  
calculated. The range error is the difference between both  
528 values ("measured range" minus "real distance"). This error is  
530 used together with the model in eq.2, and plotted in Fig.11, to  
change the weight of each particle in each filter update phase.<sub>578</sub>  
The position of the moving object is obtained by computing  
the weighted mean position of all particles. <sub>580</sub>

532 The execution time in a desktop computer (Matlab/Intel<sub>582</sub>  
i7/Windows 7) is lower than the duration of experiments, so  
the system works in real-time. The total execution time is<sub>584</sub>  
534 410 seconds for our experiment lasting 2,100 seconds, so the  
estimation process takes only 20% of the total experimentation  
536 time. Apart from the final number of particles used (2,000),  
other numbers of particles were tested (up to 100,000 particles)<sub>586</sub>  
538 but no performance improvements were appreciated. <sub>588</sub>

### B. Positioning results in our industrial conditions

540 For testing the 3D positioning performance we used the  
542 same data set used for ranging performance evaluation. So our<sub>592</sub>  
544 trajectory is the sequence of 70 test points in our workshop  
as already shown in Fig.4. We have used the particle-filter<sub>594</sub>  
546 algorithm presented above for the three UWB systems and  
the measured absolute ranges. Only the Ubisense ranges were<sub>596</sub>  
548 preprocessed in order to convert them into absolute ranges as  
explained in the first paragraph of previous section III-B (also<sub>598</sub>  
548 said at the beginning of current section IV). <sub>600</sub>

550 The positioning results are shown in Fig. 12. We start with  
552 the most accurate system, Decawave, as already known from  
ranging tests results. The Decawave trajectory is quite accurate  
554 as can be seen in Fig. 12a. The estimated trajectory in magenta  
color is mainly on top of the ground-truth path (black line). The  
556 results of Bespoon system is shown in Fig. 12b; the estimation  
is somehow reliable but not as good as in the Decawave case.  
When we use the regenerated ranges from Ubisense TDOA  
system (Fig. 12c), we obtain an estimation that is accurate only

UWB System	Mean	Median	RMS	90%
Decawave	0.49	0.39	0.59	1.09
BeSpoon	0.71	0.58	0.86	1.16
Ubisense	1.93	0.99	2.66	5.17
Ubisense (with AOA)	1.10	0.61	1.82	2.39

TABLE I. POSITIONING ERRORS (IN METERS)

at certain zones. The performance is better at the center of the working area and deteriorates at the left and right extremes.

Taking into account that Ubisense system is designed to operate using AOA information (not only TDOA), we also present the positiong results generated by the native Ubisense location engine. In this case, we do not filter or estimate position from the measurands, just plot Ubisense 3D position estimation, as presented in Fig. 12d. This solution fusing TDOA with AOA, is much better than the TDOA alone solution of Fig. 12c, however several outliers appear (long dispersed magenta lines) that spoil a bit the appearance of the estimated trajectory.

In order to better see these positioning results a Cumulative Distribution Function (CDF) is shown in Fig.13. As expected, the performance of the Decawave system is always superior to the BeSpoon system, and both better than the Ubisense TDOA case (lines red, green and blue, respectively). This can be also seen in Table I where the mean, median, 90% and RMS positioning error is computed for all cases.

The CDF result for the native Ubisense case (TDOA + AOA), dashed line in Fig.13, shows a clear improvement over the TDOA alone case. In the TDOA alone case, the number of bad measurements (error larger than 3 meters) appear to be 27% of total estimations. In the integrated solution (TDOA+AOA) the outliers are reduced to lees than 9%. However both Decawave and Bespoon systems perform better than Ubisense.

### C. Positioning precision and CRLB

In last subsection we analyzed the absolute error of position estimation versus the ground truth position. Here we inspect the precision or variance of those estimations. Theoretically, in localization systems it is possible to estimate a limit of this dispersion based on the noise of individual range measurements, and the geometry of the sensors acting as beacons for a particular number and spacial distribution. Assuming that we have an unbiased estimator (a trilateration method in our case), measurements with additive gaussian noise and enough signal-to-noise ratio, then a covariance bound can be found using the Fisher information matrix (FIM). The FIM can be computed as the Jacobian of the measurement model ( $h$ ) of a system. In our case the measurement model is  $\mathbf{z} = h(\mathbf{x}) + \epsilon$ , where  $\mathbf{z}$  are the measurements (TOA, range, etc),  $\mathbf{x}$  is the position estimation in 2D (XY) or 3D (XYZ), and  $\epsilon$  is the additive gaussian noise. The measurement model  $h(x)$  is a non-linear function that measures the distance between the mobile user's position  $x$  and the position of each of the  $N$  fixed sensors:

$$h(x) = [h_1, h_2, h_3, \dots, h_N]^T, \quad (3)$$

being  $h_i$  the individual range to a particular sensor  $i$

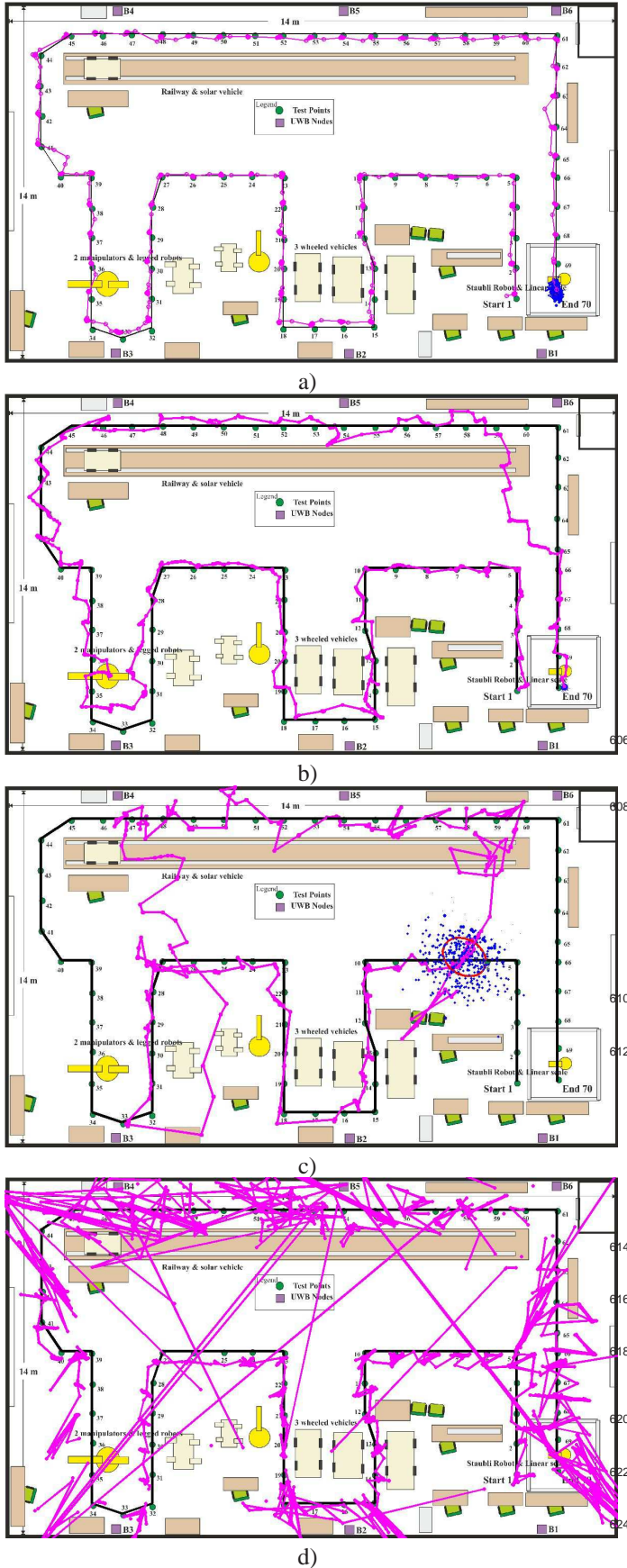


Fig. 12. Position estimation for all UWB systems: a) Decawave; b) Bespoon; c) Ubisense; d) Ubisense with AOA (no P.F.). This is a zenithal or X-Y view.  
The Black line is the ground truth trajectory; the magenta line is the estimation using a particle filter with no movement model.

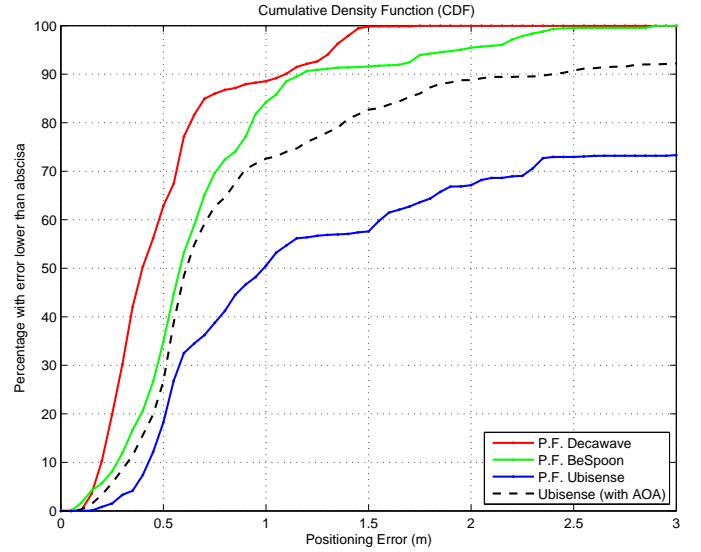


Fig. 13. Cumulative Distribution Function showing 3D positioning error ("P.F." stands for Particle Filter).

$$h_i = \|\mathbf{x} - \mathbf{x}_i\| = \sqrt{(x - x_i)^2 + (y - y_i)^2 + (z - z_i)^2} \quad (4)$$

and  $\mathbf{x}_i = x_i, y_i, z_i$  the XYZ coordinates of sensor  $i$ .

If we assume that the individual range measurement from each of the  $N$  sensors/beacons are uncorrelated, the FIM matrix can be computed as:

$$\text{FIM}(\mathbf{x}) = \sum_{i=1}^N \frac{1}{\sigma_i^2} \cdot \frac{\partial h_i}{\partial \mathbf{x}} \cdot \left( \frac{\partial h_i}{\partial \mathbf{x}} \right)^T. \quad (5)$$

The Cramer-Rao Lower Bound (CRLB) can be deduced assuming that all measurements from the  $N$  sensors have the same standard deviation ( $\sigma_i = \sigma$  for  $i = 1 \dots N$ ), by just inverting the FIM and taking the trace of its diagonal:

$$\text{CRLB} = \text{trace}\left(\text{FIM}(\mathbf{x})^{-1}\right) = \sigma^2 \cdot \left( \left( \frac{\partial h_i}{\partial \mathbf{x}} \right)^T \cdot \frac{\partial h_i}{\partial \mathbf{x}} \right)^{-1} \quad (6)$$

This CRLB is in fact proportional to the Position Dilution of Precision (PDOP) term that is commonly used in GPS community ( $\text{CRLB} = \sigma \cdot \text{PDOP}$ ). Both terms represent the amplification of noise from measurement space to the position estimation one.

In order to analyze the expected CRLB or PDOP values of our experimental setup we have prepared a graph that shows the CRLB for each of the 70 testpoints. Over this graph we also include the variance of position estimations, after removing the non-valid or far from gaussian distributions. It is important to mention that CRLB is only valid under several assumptions in the error distribution on measurements (additive, gaussian, etc), and also requires enough SNR (otherwise other bound such as Ziv-Zakai should be used [35], [36]), being that the reason for cleaning out position estimations before computing

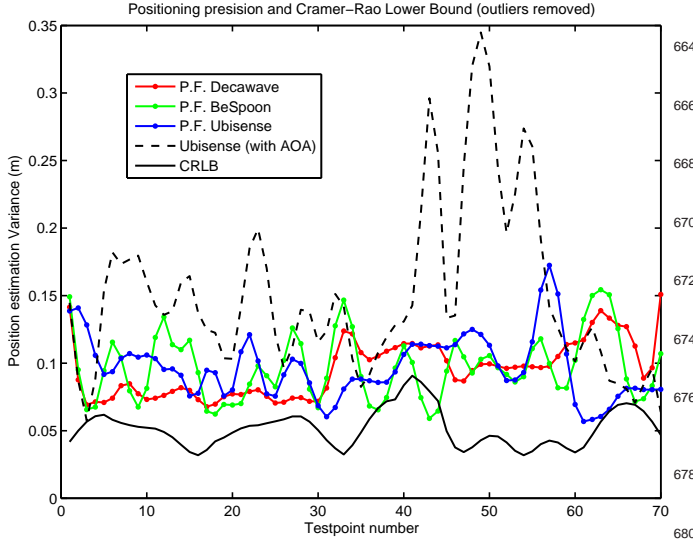


Fig. 14. Positioning precision (dispersion) and Cramer-Rao Lower Bound.  
The outliers of position estimations are removed, applying a threshold to error larger than 0.6 m (corresponds to 2 times standard deviation as seen in Fig.8 for short LOS ranges), in order to make it comparable to CRLB that assumes a gaussian error distribution.

the dispersion. In Figure 14 the experimental dispersion of the three UWB systems are compared among them and with respect to the CRLB (black continuous line at the bottom). The variance of estimations is quite noisy and not too conclusive but are in accordance with the theoretical limit. Note that the experiment, just from a geometrical point of view, did not include any region with a poor conditioning. Only test points from 39 to 44 were more sensitive to noise due to a larger dilution of precision (a maximum of PDOP of 4.02 for point 41) that corresponds to points outside the rectangle enclosed by sensors positions.

## V. CONCLUSIONS

We have presented an experimental evaluation of three commercially available UWB positioning systems: Ubisense, Decawave and Bespoon. The evaluation has been done in a NLOS environment similar to an industrial warehouse with diverse equipment (robots, vehicles, railways, etc.) which perturbs UWB radio propagation. Under these conditions, the performance of Decawave system is slightly better than the BeSpoon system and significantly more reliable, in terms of accuracy and outlier content, than the Ubisense system.

The conclusion that Decawave is more accurate than Bespoon system is the same that was already obtained in [24] under free-of-obstacle LOS conditions and when the UWB radio propagated throughout some walls in an apartment-size space. These results are somehow logical since Decawave is using a more advanced antenna system than the Bespoon equipment, which is a miniature implementation within a small tag, and with part of the UWB system integrated together with the electronics of a mobile phone.

The performance results for the Ubisense equipment are lower than Decawave and Bespoon, and this occurs in case of only using TDOA data and also when using the integrated localization solution that fuses TDOA and AOA. The potential

advantage of the costly Ubisense equipment, with bulky array antennas that even require cables for synchronization and powering, are not translated into a better accuracy. The number of outlying measurements makes difficult to obtain reliable position estimation under our testing conditions. That findings correlate with some previous works using the same Ubisense equipment [37], in that case using 4 sensors of series 7000 in a testing space of 3 by 3 meters. There, it was found that the TDOA measurements were also too noisy, so in order to reduce positioning errors down to 0.5 m, a filtering with odometry-based motion models was needed [37], [34]. Apart from that, and comparing the two measurands available with Ubisense (TDOA and AOA), we can say that the AOA is more informative and accurate for correct positioning, and contains fewer outliers, than TDOA data.

The results of this comparison show a superior performance of Decawave over Bespoon, and both behaves better than Ubisense equipment. It is fair to mention that Ubisense system dates from 2009 and Bespoon from 2015, while Decawave is from 2016, and now some new versions are available for Ubisense (Dimension4) and Bespoon (centralized RTLS & Inverted 3D), that could probably improve the results obtained in the current comparison.

Future research will consider the use of millimeter-accurate positioning systems for outdoor long-range tests (such as total stations or Differential RTK-GPS). The use of this systems in dynamic scenarios for vehicle location and tracking, making use of fusion techniques combining UWB with inertial or other motion information is another topic of future study.

## ACKNOWLEDGMENT

The authors thank the financial support received from projects: LORIS (TIN2012-38080-C04-04), TARSUS (TIN2015-71564-C4-2-R (MINECO/FEDER)) and REPNIN (TEC2015-71426-REDT).

## DISCLAIMER

Statements and opinions given in this article are the expression of the authors.

## REFERENCES

- [1] R. Mautz, *Indoor Positioning Technologies*. PhD thesis, ETH Zurich, 2012.
- [2] Y. Gu, A. Lo, and I. Niemegeers, "A Survey of Indoor Positioning Systems for Wireless Personal Networks," *IEEE Communications Surveys and Tutorials*, vol. 11, no. 1, pp. 13–32, 2009.
- [3] J. Hightower and G. Borriello, "Location Systems for Ubiquitous Computing," *Computer*, vol. 34, no. 8, pp. 57 – 66, 2001.
- [4] N. Ravi, P. Shankar, A. Frankel, A. Elgammal, and L. Iftode, "Indoor Localization Using Camera Phones," in *WMCSA '06 Proceedings of the Seventh IEEE Workshop on Mobile Computing Systems & Applications*, pp. 1–16, 2006.
- [5] A. R. Jiménez, F. Seco, J. C. Prieto, and J. Guevara, "A comparison of Pedestrian Dead-Reckoning algorithms using a low-cost MEMS IMU," in *2009 IEEE International Symposium on Intelligent Signal Processing*, (Budapest), pp. 37–42, 2009.
- [6] R. Mautz, "The challenges of indoor environments and specification on some alternative positioning systems," in *Positioning, Navigation and Communication WPNC'09*, (Hannover), pp. 29–36, 2009.

- [7] L. E. Miller, "Indoor Navigation for First Responders : A Feasibility Study," Tech. Rep. February, National Institute of Standards and Technology, Gaithersburg, USA, 2006.
- [8] E. Foxlin, "Pedestrian tracking with shoe-mounted inertial sensors," *IEEE Computer Graphics and Applications*, vol. 25, no. 6, pp. 38–46, 2005.
- [9] A. R. Jiménez, F. Seco, J. C. Prieto, and J. Guevara, "Indoor Pedestrian Navigation using an INS/EKF framework for Yaw Drift Reduction and a Foot-mounted IMU," in *WPNC 2010: 7th Workshop on Positioning, Navigation and Communication*, (Dresden), pp. 135 – 143, 2010.
- [10] A. R. Jimenez, F. Seco Granja, J. C. Prieto Honorio, J. I. Guevara Rosas, and A. Jiménez, "Accurate Pedestrian Indoor Navigation by Tightly Coupling a Foot-mounted IMU and RFID Measurements," *IEEE Transactions on Instrumentation and Measurement*, vol. 61, pp. 178–189, jan 2012.
- [11] R. Harle, "A Survey of Indoor Inertial Positioning Systems for Pedestrians," *IEEE Communications Surveys and Tutorials*, no. December 2012, pp. 1–13, 2013.
- [12] J. Wilson and N. Patwari, "Radio Tomographic Imaging with Wireless Networks," *IEEE Transactions on Mobile Computing*, vol. 9, pp. 621–632, may 2010.
- [13] B. Wagner and D. Timmermann, "Approaches for Device-free Multi-User Localization with Passive RFID," in *IEEE Int Conf on Indoor Positioning and Indoor Navigation*, pp. 28–31, 2013.
- [14] O. Kaltiokallio, M. Bocca, and N. Patwari, "A Multi-Scale Spatial Model for RSS-based Device-Free Localization," *arXiv preprint arXiv:1302.5914*, pp. 1–13, 2013.
- [15] F. Seco, A. R. Jimenez, and F. Zampella, "Fine-Grained Acoustic Positioning with Compensation of CDMA Interference," in *IEEE Int. Conf. on Industrial Technology (ICIT)*, (Seville), pp. 3418 – 3423, 2015.
- [16] F. Seco, J. C. Prieto, A. R. Jimenez, and J. Guevara, "Compensation of multiple access interference effects in CDMA-based acoustic positioning systems," *IEEE Transactions on Instrumentation and Measurement*, vol. 63, no. 10, pp. 2368–2378, 2014.
- [17] J. C. Prieto, C. Croux, and A. R. Jimenez, "RoPEUS: A new robust algorithm for static positioning in ultrasonic systems," *Sensors*, vol. 9, no. 6, pp. 4211–4229, 2009.
- [18] J. C. Prieto, A. R. Jiménez, J. Guevara, J. L. Ealo, F. Seco, J. O. Roa, and F. Ramos, "Performance Evaluation of 3D-LOCUS Advanced Acoustic LPS," *IEEE Transactions on Instrumentation and Measurement*, vol. 58, no. 8, pp. 2385–2395, 2009.
- [19] J. Tiemann, F. Schweikowski, and C. Wietfeld, "Design of an UWB Indoor-Positioning System for UAV Navigation in GNSS-Denied Environments," in *International Conference on Indoor Positioning and Indoor Navigation (IPIN)*, pp. 1–7, 2015.
- [20] I. Guvenc, C. C. Chong, and F. Watanabe, "NLOS identification and mitigation for UWB localization systems," *IEEE Wireless Communications and Networking Conference, WCNC*, pp. 1573–1578, 2007.
- [21] L. Zwirello, T. Schipper, M. Jalilvand, and T. Zwick, "Realization Limits of Impulse-Based Localization System for Large-Scale Indoor Applications," *IEEE Transactions on Instrumentation and Measurement*, vol. 64, no. 1, pp. 39–51, 2015.
- [22] A. R. Jiménez, J. C. Prieto, J. L. Ealo, J. Guevara, and F. Seco, "A computerized system to determine the provenance of finds in archaeological sites using acoustic signals," *Journal of Archaeological Science*, vol. 36, no. 10, pp. 2415–2426, 2009.
- [23] A. Cazzorla, G. D. Angelis, A. Moschitta, M. Dionigi, F. Alimenti, and P. Carbone, "A 5 . 6-GHz UWB Position Measurement System," *IEEE Transactions on Instrumentation and Measurement*, vol. 62, no. 3, pp. 675–683, 2013.
- [24] A. R. Jimenez and F. Seco, "Comparing Decawave and Bespoon UWB location systems: indoor / outdoor performance analysis," in *6 Int. Conference on Indoor Positioning and Indoor Navigation (IPIN)*, no. October, pp. 4–7, 2016.
- [25] D. Dardari, A. Conti, U. Ferner, A. Giorgetti, and M. Z. Win, "Ranging With Ultrawide Bandwidth Signals in Multipath Environments," *Proceedings of the IEEE*, vol. 97, no. 2, pp. 404–426, 2009.
- [26] A. D. Angelis, S. Member, M. Dionigi, A. Moschitta, R. Giglietti, P. Carbone, and S. Member, "Characterization and Modeling of an Experimental UWB Pulse-Based Distance Measurement System," *IEEE Transactions on Instrumentation and Measurement*, vol. 58, no. 5, pp. 1479–1486, 2009.
- [27] M. Wylie and J. Holtzman, "The non-line of sight problem in mobile location estimation," *Proceedings of ICUPC - 5th International Conference on Universal Personal Communications*, vol. 2, no. 3, pp. 3–7, 1996.
- [28] A. Rabbachin, B. Denis, I. Oppermann, and C. E. A. Leti, "ML Time-of-Arrival estimation based on low complexity UWB energy detection," in *IEEE Int. Conf. on Ultra-Wideband*, no. 1, (Waltham, MA), pp. 599–604, 2006.
- [29] P. C. Chen, "A non-line-of-sight error mitigation algorithm in location estimation," *IEEE Wireless Communications and Networking Conference, WCNC*, vol. 1, pp. 316–320, 1999.
- [30] F. G. H. Nurminen, T. Ardesiri, R. Piche, "A NLOS-robust TOA positioning filter based on a skew- t measurement noise model," in *International Conference on Indoor Positioning and Indoor Navigation (IPIN)*, no. October, pp. 13–16, 2015.
- [31] H. Nurminen, T. Ardesiri, R. Piché, and F. Gustafsson, "Robust Inference for State-Space Models with Skewed Measurement Noise," *Signal processing letters*, vol. 22, no. 11, pp. 1898–1902, 2015.
- [32] W. Suski, S. Banerjee, and A. Hoover, "Using a Map of Measurement Noise to Improve UWB Indoor Position Tracking," *IEEE Transactions on Instrumentation and Measurement*, vol. 62, no. 8, pp. 2228–2236, 2013.
- [33] A. Prorok, P. Tom, and A. Martinoli, "Accommodation of NLOS for Ultra-Wideband TDOA Localization in Single- and Multi-Robot Systems," in *Indoor Positioning and Indoor Navigation (IPIN), 2011 International Conference on*, 2011.
- [34] A. Prorok, L. Gonon, and A. Martinoli, "Online Model Estimation of Ultra-Wideband TDOA Measurements for Mobile Robot Localization," in *Robotics and Automation (ICRA), 2012 IEEE International Conference on*, 2012.
- [35] J. Ziv and M. Zakai, "Some Lower Bounds on Signal Parameter Estimation 1 T," *IEEE Transactions on Information Theory*, vol. 15, no. 3, pp. 386–391, 1969.
- [36] S. Kay, *Fundamentals of Statistical Signal Processing, Vol I: Estimation theory*. Kay1993: Prentice Hall, 1993.
- [37] A. Prorok, A. Arfire, A. Bahr, J. R. Farserotu, and A. Martinoli, "Indoor Navigation Research with the Khepera III Mobile Robot : An Experimental Baseline with a Case-Study on Ultra-Wideband Positioning," no. September, pp. 15–17, 2010.